Offshore permafrost decay and massive seabed methane escape in water depths >20 m at the South Kara Sea shelf

Alexey Portnov,[1,2] Andrew J. Smith,[1,2] Jürgen Mienert,[1,2] Georgy Cherkashov,[3] Pavel Rekant,[3] Peter Semenov,[3] Pavel Serov,[3] and Boris Vanshtein[3]

Received 14 May 2013; revised 8 July 2013; accepted 10 July 2013.

[1] Since the Last Glacial Maximum (~19 ka), coastal inundation from sea-level rise has been thawing thick subsea permafrost across the Arctic. Although subsea permafrost has been mapped on several Arctic continental shelves, permafrost distribution in the South Kara Sea and the extent to which it is acting as an impermeable seal to seabed methane escape remains poorly understood. Here we use >1300 km of high-resolution seismic data to map hydroacoustic anomalies, interpreted to record seabed gas release, on the West Yamal shelf. Gas flares are widespread over an area of at least 7500 km^2 in water depths >20 m. We propose that continuous subsea permafrost extends to water depths of ~20 m offshore and creates a seal through which gas cannot migrate. This Arctic shelf region where seafloor gas release is widespread suggests that permafrost has degraded more significantly than previously thought.
Citation: Portnov, A., A. J. Smith, J. Mienert, G. Cherkashov, P. Rekant, P. Semenov, P. Serov, and B. Vanshtein (2013), Offshore permafrost decay and massive seabed methane escape in water depths >20 m at the South Kara Sea shelf, *Geophys. Res. Lett.*, *40*, doi:10.1002/grl.50735.

1. Introduction

[2] During the extreme cold stages of the Late Pleistocene (marine oxygen isotope stages (MIS) 2 and 4), thick permafrost and gas-hydrate deposits developed within coastal sediments across the Arctic [*Khimenkov and Brushkov*, 2003]. Since the beginning of the last transgression (~19 ka), warm ocean water flooded these sediments due to sea-level rise (~120 m), raising the annual temperature of the former tundra surface by as much as 15°C [*Taylor*, 1991]. As a result, permafrost and gas hydrates have been melting and releasing massive quantities of methane into the ocean and atmosphere, possibly accelerating global warming [*Bohannon*, 2008; *Shakhova et al*., 2010a].

[3] Subsea permafrost degradation and associated methane release have been mapped on the East Siberian margin [*Shakhova et al*., 2010b], the Beaufort Sea continental shelf [*Brothers et al*., 2012; *Paull et al*., 2011], and the Canadian Beaufort [*Hunter et al*., 1978]. *Rekant and Vasiliev* [2011] use seismic reflection data to map subsea permafrost in the Kara Sea and suggest that the extent of permafrost is limited approximately by the 60 m isobath (Figure 1). This study, however, interprets a prominent subseabed reflector and underlying acoustically transparent layer as permafrost, but these acoustic features could instead result from the presence of free gas [*Rokos et al*., 2001]. Furthermore, offshore drilling data recovered permafrost in only ~15% of cores in water depths >20 m, suggesting that continuous permafrost does not extend deeper [*GEOS*, 1997; *Melnikov and Spesivtsev*, 1995]. A map of subsea permafrost in the Kara Sea that can reconcile both seismic and drilling observations has yet to be produced.

[4] Here we map hydroacoustic anomalies, interpreted to record the release of gas bubbles at the seafloor, on >1300 km of high-resolution seismic (HRS) data on the West Yamal shelf in the Kara Sea (Figure 1). These anomalies occur over an area of at least 7500 km^2 in water depths deeper than 20 m. Since continuous permafrost creates an impermeable seal through which gas cannot migrate [*Shakhova et al*., 2010b], we propose that it extends offshore to water depths of ~20 m. The offshore extent of permafrost in the Kara Sea is strikingly similar to that observed on the U.S. Beaufort Sea shelf [*Brothers et al*., 2012], suggesting that the two regions have experienced similar inundation histories since the Last Glacial Maximum. These results contribute towards a pan-arctic understanding of permafrost degradation.

2. Geologic Setting

[5] The coastal shelf offshore the West Yamal Peninsula is between 100–120 km wide from the shoreline to the 100 m isobath in the southern Kara Sea and 70–80 km wide to the North. Shallow water depths (<20 m) extend up to 80 km offshore in the South but only 20–30 km offshore to the North (Figure 1). There is not significant seafloor relief across the shelf, except for minor troughs likely associated with ice-scouring processes [*Sherbakov et al*., 2010]. The upper sedimentary cover is composed of 150–200 m thick marine and alluvial-marine deposits of Pleistocene-Holocene age [*Melnikov and Spesivtsev*, 1995]. Approximately 40 m thick clays and silts of pre-Weichselian age are separated from overlying deposits by an unconformity, dated to be between 100 and 120 ka. Above the unconformity, interbedded clays, silts, and sands compose a 5–25 m thick section of Middle Weichselian-Holocene age (MIS 4–MIS 1). Holocene clays, silts, and sands with 1–5 m thickness overlie this section. Regional faults of Late Permian to Jurassic age and shallow neotectonic faults trend NE-SW and NW-SE across the study area [*Sherbakov et al*., 2010].

Additional supporting information may be found in the online version of this article.

[1]Centre for Arctic Gas Hydrate, Environment and Climate, University of Tromsø, Tromsø, Norway.
[2]Department of Geology, University of Tromsø, Tromsø, Norway.
[3]I.S. Gramberg VNIIOkeangeologia, Saint Petersburg, Russia.

Corresponding author: A. Portnov, Centre for Arctic Gas Hydrate, Environment and Climate, University of Tromsø, Dramsveien 201, NO-9037 Tromsø, Norway. (portnovalexey@gmail.com)

©2013. American Geophysical Union. All Rights Reserved.
0094-8276/13/10.1002/grl.50735

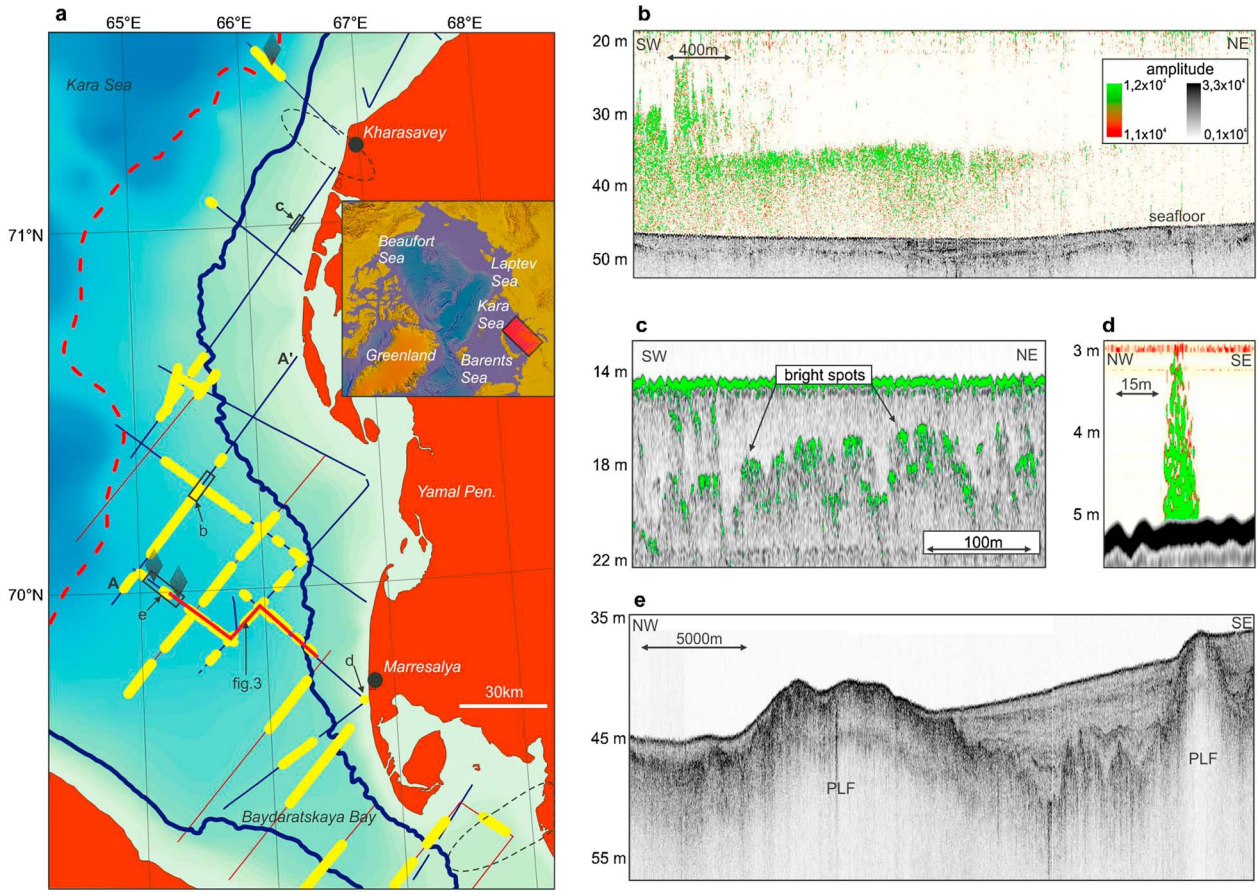

Figure 1. (a) Distribution of gas flares (yellow lines) in the water column offshore the West Yamal Peninsula at the South Kara Sea shelf (location shown on inset). Flares were mapped using HRS data from 2010 (brown lines) and 2012 (blue lines). The flares are limited approximately to water depths >20 m (solid blue line). Dotted red line shows the extent of permafrost mapped by *Rekant and Vasiliev* [2011]. Solid red line shows the transect displayed in Figure 3a. Dotted black ellipses show the location of previous drilling studies that recovered permafrost [*GEOS*, 1997; *Melnikov and Spesivtsev*, 1995]. (b) Gas flares were observed as continuous fronts that were >60 km long and that extended 20–25 m above the seafloor. Two-way traveltime was converted to depth assuming an acoustic velocity of 1.5 km s^{-1} for all seismic reflection profiles. (c) Bright spots below the seafloor are interpreted to record the presence of gas and/or ice. (d) A focused, intermittent flare was observed extending ~2 m above seafloor in water depths of ~5.5 m. (e) Three transparent mounds that pierced through seafloor sediments were observed in the study area (grey diamonds). These features are similar in appearance to the pingo-like features (PLF) characterized by *Paull et al*. [2007] on the Beaufort shelf.

[6] According to ice sheet reconstructions, the West Yamal shelf was not glaciated during the Late Weichselian [*Polyak et al*., 2008]. As a result, the continental shelf was exposed to continuous subaerial conditions, leading to the development of a several hundred meter thick permafrost layer. Onshore drilling has recorded permafrost layers >300 m thick in coastal areas [*Melnikov and Spesivtsev*, 1995] and further inland on the Yamal Peninsula [*Skorobogatov et al*., 1998]. Offshore drilling has also recorded relict and modern permafrost in water depths up to 115 m offshore, although the majority of permafrost was found to be in wells with water depths <20 m [*GEOS*, 1997].

3. Methods

[7] We acquired ~700 km of HRS lines during a cruise aboard the *R/V Neotrazimiy* operated by I.S. Gramberg VNIIOkeangeologia in August–September 2012 to the West Yamal shelf. HRS lines were collected in NW-SE and NE-SW trending lines with a line spacing of 30–40 km (Figure 1). In addition, we incorporate ~600 km of HRS data, acquired in 2010 in the same region [*Sherbakov et al*., 2010]. The surveys spanned an area from the Baydaratskaya Bay in the South to Kharasavey in the North. The data were acquired with the sub-bottom chirp profiler EdgeTech 3100 SB-216S that operates at a range of frequencies (2–16 kHz). These data provide at best sub-bottom penetration of 80 m in clay and yield a vertical resolution of 2–20 cm for favorable weather conditions. However, due to the high sea states during the cruise, the data provide at best ~0.5–1 m vertical resolution.

[8] The HRS data were used to characterize the upper sedimentary cover of the West Yamal shelf. Because of the high-impedance contrast between water and free gas and the high frequency of our sound source, the HRS data were also used to detect gas bubble emissions from the seafloor. These emissions are imaged as "acoustic flares" in the seismic data. Flares are first-order proof for active gas seepage from the seafloor [*Greinert et al*., 2010]. Flares can be produced from a single bubble stream or from multiple streams rising from several adjacent seep locations. Therefore, the magnitude of

bubble release to the seabed or atmosphere cannot be quantified with this technique. HRS data were imported and interpreted in The Kingdom Suite software.

[9] We used a marine box corer to sample sediments in the first ~0.4 m below seafloor at 190 geological stations. The lithology of sediments was described onboard visually. To confirm that acoustic flares were in fact produced by gas bubbles, we also made measurements of methane concentrations in the water column ~0.5 m above the seabed. Water volumes of ~8 L were recovered at each water sample station. The gas fraction from the water samples was extracted onboard using a supersonic ejector technique. The water sample is degassed in the supersonic ejector set SUOK-DG; the extracted gas phase is evacuated into a 15 mL vial stoppered by butyl rubber stoppers. Methane was measured in an onshore VNIIOkeangeologia lab using Shimadzu GC 2014 equipped with a flame ionization detector. A wide-bore capillary column Restek Aluminia (0.53 mm; 50 m) was employed to separate methane from other hydrocarbon gases. The carrier gas was He that flowed at a rate of 20 mL/min. Peaks were calibrated against certified standard gas mixtures. Mean methane concentrations were determined by averaging 193 individual measurements across our study area.

4. Results

4.1. Gas Flares

[10] Hydroacoustic flares, interpreted as gas bubbles in the water column, were widespread throughout the study area (Figures 1a, 1b, and 3a). Flares were observed at a range of intensities, suggesting that gas flux across the shelf is highly variable and that some regions experience more intense emissions than others. Flares were often deflected laterally (Figures 1b and 3a). The direction of this deflection was different across the study area as a result of the complex interplay of regional and tidal currents [*GEOS*, 1997; *Sherbakov et al*., 2010]. Flares extended to heights of up to 20–25 m above seafloor (Figures 1b and 3a). Most flares were limited to water depths >20 m across the study area; however, a few flares were discovered in the Baydaratskaya Bay in shallower water depths (10–20 m) (Figure 1a). The distribution of flares in 2012 agrees with their distribution in 2010 [*Sherbakov et al*., 2010] (Figure 1a), suggesting that gas is being released continuously over an area of at least 7500 km^2. On several HRS lines, a 30–60 km gas front was observed extending from the 20 m isobath to water depths >40 m (Figures 1a and a). In the northern part of the study area, flares were limited to water depths >30 m (Figure 1a).

[11] A single-focused gas flare was found ~1.5 km from the coastline near Marresalya in ~6 m water depth (Figure 1d). This flare was ~2 m high and ~15 m wide. Gas expulsion at this site appears to be intense since the seismic amplitudes of the flare reflection were similar to those observed below the seafloor. However, subsequent passes over this location ~1 month later failed to detect any flare, indicating that gas expulsion at the site is intermittent over relatively short (monthly) timescales.

4.2. Seismic Observations in Upper Sedimentary Cover

[12] Enhanced subseabed reflections or "bright spots" were ubiquitous across the study area. They were in water depths 6–50 m (Figure 1c), and there appeared to be no systematic pattern in their occurrence. In the Kara Sea, these reflections have been separately interpreted to record the presence of gas-saturated sediments [*Rokos et al*., 2001] and ice-bearing sediments disturbed from cryogenic deformation [*Bondarev et al*., 1999]. Our chirp data were recorded as enveloped amplitudes and do not show reflection polarity; therefore, they cannot be used to distinguish between negative-polarity reflections from gas-charged sediments and positive-polarity reflections from ice-bearing sediments.

[13] Acoustically transparent zones, where seismic energy is not coherently reflected back to the receiver and where subseabed reflectors are not clearly imaged within sediments, were also widespread throughout the study area. One of these zones is at least 250 m wide and extends vertically from the seafloor to depths greater than we can resolve with our data (Figure 3a, red inset). This "wipe-out" zone is strikingly similar in size and character to gas chimneys, vertically oriented zones of gas migration which have been observed in conventional seismic data around the world [e.g., *Hovland and Judd*, 1988; *Wood et al*., 2002].

[14] Broad zones of acoustic transparency were also present at the seafloor and in the subseabed (Figures 1e and 3a). These zones exist in all water depths, and they occur at the seafloor and at depths up to ~10 m below seafloor. The exact geologic nature of these zones is ambiguous. They may be produced by the absorption of acoustic energy due to the presence of gas or the scattering of energy from the presence of unevenly distributed accumulations of gas, ice-bearing sediments, calcium carbonate, or stratal disruptions from intense fluid flux [e.g., *Wood et al*., 2002]. Previous investigations have directly observed ice-bearing sediments and encountered significant accumulations of free gas in the subsurface across the West Yamal shelf [*Melnikov and Spesivtsev*, 1995]. The widespread coexistence of these phenomena suggests that a combination of frozen sediments and free gas may create these broad zones of acoustic transparency.

4.3. Pingo-Like Features

[15] At three locations in our study area, we observed distinct ovoid, positive-relief features that were elevated 5–10 m above the surrounding seafloor and were at least 1–5 km in diameter (Figures 1e and 3a). These features emanate from within 10–20 m deep bathymetric depressions that are filled with flat-lying sediments of Upper Pleistocene to Holocene age that fan downwards toward the center of the mounds (Figure 1e). We observed weak gas flares above two out of three of the features, indicating that they were not expelling significant quantities of gas. These features are strikingly similar in size and appearance to the pingo-like features (PLFs) described by *Paull et al*. [2007] in the Beaufort Sea, to terrestrial pingos that have been observed along coastal plains [*Shearer et al*., 1971], and to diapir-like features documented in the Pechora Sea [*Bondarev et al*., 2002]. However, in contrast to observations made by *Paull et al*. [2011], we did not detect significant gas expulsion from these transparent domes. This apparent lack of activity, however, may be due to passes over inactive areas of the mounds or during periods of inactivity.

[16] The origin of these PLFs remains elusive. Previous studies have suggested that they formed as a result of base-level rise over terrestrial pingos [*Kopf*, 2002], overpressures generated during gas-hydrate dissociation [*Paull et al*., 2007], or free-gas accumulation beneath melting permafrost [*Bondarev et al*., 2002]. The acoustic transparency of the

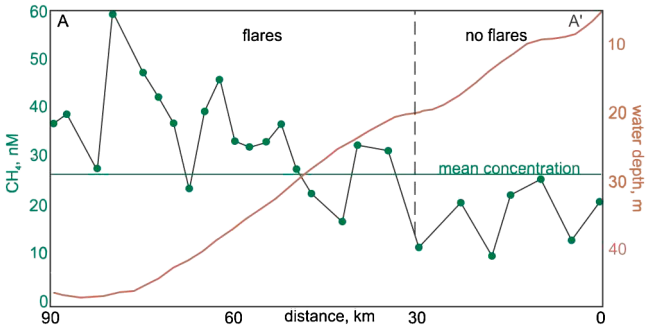

Figure 2. Methane concentrations measured (green) in the bottom-water layer (~0.5 m above seafloor) along a ~90 km transect (red line). Location of transect is shown in Figure 1a (A–A′). Methane concentrations increase significantly in water depths >20 m, coincident with the onset of gas flares. Error (~ ±1.4 nM) is smaller than symbol size at all measurements.

core of PLFs in the Kara Sea suggests that either gas and/or ice are present in the subsurface; however, future-focused drilling needs to be conducted to decipher the processes present and to determine whether their origin is the same as those in the Beaufort and Pechora Seas.

4.4. Methane Concentrations

[17] Throughout the study area, methane concentrations in water just above the seafloor were higher than "open ocean" background values in the Arctic (<4 nM) [*Damm et al.*, 2007]. The methane concentrations showed a systematic increase in values along a 90 km transect extending from the near shoreline to 75 km offshore (Figure 2). Methane concentrations at water depths <20 m have values that were significantly less than the mean concentration (~27 nM). However, at the 20 m isobath, there is a sharp increase in methane concentrations to values that are consistently higher than the mean (Figure 2). Although we observe an increase in methane concentrations with increasing water depths, there is significant variability in concentrations across the 90 km long transect, which is similar to the inconsistent flare intensity observed across the study area (Figures 2 and 3a).

5. Discussion

[18] Previous works have proposed that permafrost in the Kara Sea and other Arctic marine basins extends to deeper water depths, i.e., of up to 100 m and to offshore distances as great as the outer shelf edge and that this widely distributed permafrost layer creates a seal that hydrocarbons cannot bypass [*Paull et al.*, 2011; *Romanovskii and Hubberten*, 2001]. In contrast, we show that the West Yamal shelf is leaking significant quantities of gas at much shallower water depths (20–50 m) and over an area of at least 7500 km^2, suggesting that a continuous permafrost seal is much less extensive and does not extend to water depths >20 m. However, a chaotic distribution of acoustically transparent zones in 20–50 m water depth and previous drilling data suggest that some erratic occurrences of ice-bearing sediments may exist in deeper water depths. These ice-bearing

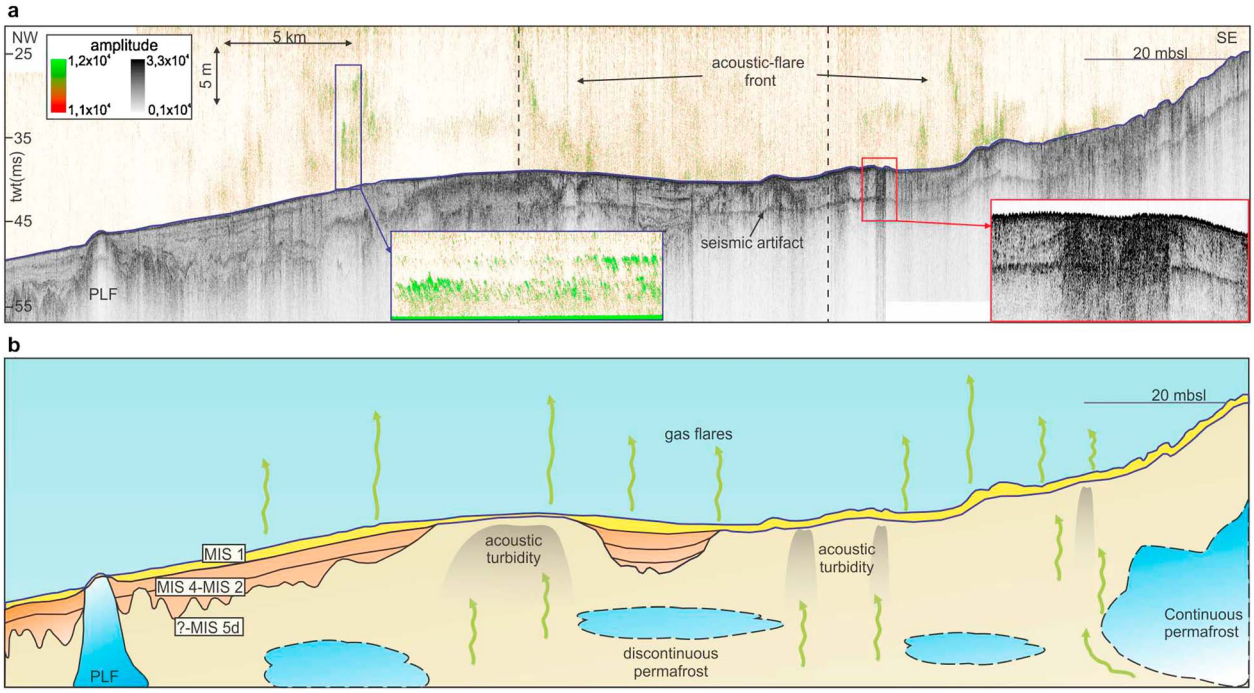

Figure 3. (a) HRS profile shows a >30 km gas flare front above the upper sedimentary cover. The location of the profile is shown in Figure 1a (solid red line). Inset with a blue frame highlights gas flares emanating from seabed. Inset with red frame shows a ~250 m wide transparent zone interpreted as a gas chimney. The event labeled as a "seismic artifact" is a sea-surface ghost reflection related to the tow depth of the chirp fish. (b) We envision that a continuous subseabed permafrost body limits the occurrence of gas flares to depths >20 m. Discontinuous ice-bearing sediment masses are likely present in deeper water depths; however, they do not create an effective seal for gas migration. Gas (green arrows) may be produced from thermogenic sources at depth, from disassociating gas hydrates, microbial processes in shallow sediments, or microbial action of organic carbon newly released from thawing permafrost.

sediments likely do not form a continuous body, and therefore do not act as an effective and widespread seal for gas migration.

[19] Although flares similar to those that we observe are most often attributed to seabed gas release [e.g., *Westbrook et al*., 2009], there is still uncertainty that the acoustic flares we map are indeed caused by gas bubbles. Backscatter signals in the water column can also be produced by rising gas-hydrate particles, oil droplets, sediment particles, or zooplankton blooms [*Merewether et al*., 1985; *Robinson and Goómez-Gutieérrez*, 1998]. However, the majority of producing reservoirs in the region are gas or gas condensate fields that produce little to no oil [*Stupakova*, 2011]. Moreover, given bottom-water temperatures in the region (−1.7°C to 5°C) [*GEOS*, 1997; *Sherbakov et al*., 2010] and assuming hydrostatic pressure conditions, seawater salinity, and pure methane gas composition, gas hydrates are not stable at the seabed and near subseabed [*Sloan*, 1998]. Furthermore, the continuous and widespread flare activity that we observe from 2010 to 2012 cannot be reconciled with the fast and abrupt (hourly) timescale over which zooplankton blooms occur [*Robinson and Goómez-Gutieérrez*, 1998]. We therefore are confident that the flares observed are produced by gas bubbles. This interpretation is further corroborated by the systematic increase in methane concentrations in the water column at water depths >20 m, suggesting that methane is being delivered to the water column at locations where flares are present. Furthermore, the backscatter pattern and linear features of flares observed in HRS data are similar to those that have been observed at other shallow gas-venting locations [*Westbrook et al*., 2009] and during in situ experiments [*Polikarpov et al*., 1989].

[20] We suggest that gas release is limited by the 20 m isobath because continuous subsea permafrost extends offshore to these depths (Figure 3b). Seafloor gas emissions, however, can also be controlled by structural (e.g., faults) and lithological (e.g., permeable sands) phenomena [*Tréhu et al*., 2004; *Vadakkepuliyambatta et al*., 2013]. But, the presence of gas flares on the West Yamal shelf does not coincide with the locations of faults, and the basin-wide distribution of seafloor sands and silts is not correlated to the location of flares (Figure S1). These observations suggest that a different geologic phenomenon controls gas expulsion at the seafloor. Due to the recovery of permafrost in ~85% of cores in water depths <20 m [*GEOS*, 1997] and to identical permafrost extents in other Arctic basins [*Brothers et al*., 2012], we favor the interpretation that continuous permafrost is creating a gas seal and controlling the regional distribution of flares.

[21] In water depths >20 m, widespread zones of acoustic transparency, PLFs, and previous drilling data suggest that ice-bearing sediments are present. The nonrecovery of permafrost in the majority of cores, however, suggests that ice-bearing sediments in these depths do not form a continuous body [*GEOS*, 1997]. Furthermore, the widespread occurrence of seafloor gas emissions in these water depths indicates that permafrost is not creating a gas trap. We therefore envision that continuous permafrost extends to water depths of ~20 m and that discontinuous ice-bearing sediments extend further offshore (Figure 3b). These discontinuous masses of ice-bearing sediments may be relict permafrost from the last regression or older regressions [*Khimenkov and Brushkov*, 2003]. Conversely, these sediment-ice bodies may have formed from sediment-ice mobilizations or seasonal-to-decadal temperature changes that have occurred recently at the seabed [*Khimenkov and Brushkov*, 2003]. It is unclear how far offshore these discontinuous bodies of ice-bearing sediments extend, but based on drilling data, they likely reach water depths of up to 115 m [*Melnikov and Spesivtsev*, 1995].

[22] Although flares are limited to water depths >20 m on most of the West Yamal shelf, flares to the North near Kharasavey are limited to deeper water depths (>30 m) and flares near Baydaratskaya Bay are present in shallower water depths (10–20 m). These regional variations in flare distribution suggest that continuous permafrost may extend to deeper water depths near Kharasavey and to shallower water depths within the Baydaratskaya Bay. Seafloor temperature measurements from 1980–2010 show that Baydaratskaya Bay experiences on average higher sea-bottom temperatures than regions further North [*GEOS*, 1997; *Sherbakov et al*., 2010], which would accelerate permafrost degradation. Cooler bottom-water temperatures near Kharasavey may explain a larger extent of impermeable permafrost and thus the deeper limit of gas flares. In addition, the steeper topography of the shelf near Kharasavey may explain the deeper offshore extent of permafrost, since shelf steepness affects the rate of inundation during sea-level rise and the degree of warming experienced by underlying permafrost [*Brothers et al*., 2012; *Khimenkov and Brushkov*, 2003].

[23] The implications of our study are two-fold. First, we show that the extent of continuous permafrost on the West Yamal shelf likely does not extend to water depths >20 m and that this depth is far shallower than previously thought [*Rekant and Vasiliev*, 2011]. This permafrost extent is strikingly similar to that which was mapped by *Brothers et al*. [2012] on the Beaufort shelf, suggesting that the two basins have experienced similar inundation histories since the Late Pleistocene. Conversely, we show that seafloor gas expulsion on the West Yamal shelf is extensive and occurs over an area of at least 7500 km^2. Studies on the East Siberian shelf have shown that massive amounts of methane (7.98 Tg C-CH_4 yr^{-1}) are being released over an area of 2.1×10^6 km^2 to the atmosphere from seafloor sediments previously sealed by impermeable permafrost [*Shakhova et al*., 2010a; *Shakhova et al*., 2010b]. Although we cannot presently constrain oceanic or atmospheric methane fluxes in our study, the presence of extensive gas venting and permafrost degradation on the West Yamal shelf suggests that significant methane fluxes may also be present in the Kara Sea now and even more so in a future warming scenario.

6. Conclusions

[24] At the West Yamal shelf seafloor, gas expulsion occurs over an area of at least 7500 km^2, and it is limited approximately to water depths >20 m. Continuous subseabed permafrost extends to water depths of ~20 m offshore and creates a seal through which gas cannot migrate. Discontinuous permafrost may extend further offshore in up to 115 m water depth. This study provides one of the key examples of an Arctic marine shelf where seafloor gas release is widespread and where permafrost degradation is an ongoing process.

[25] **Acknowledgments.** The research is part of the Centre of Excellence: Arctic Gas Hydrate, Environment and Climate (CAGE) funded by the Norwegian Research Council (grant 223259). A. Portnov is supported by a Statoil fellowship through the University of Tromsø. The field research was funded by the Federal Subsoil Resources Management Agency of Russia (object 70-113: "Regional geologic-geophysical explorations at Yamal sector of South Kara Sea shelf"). We thank B. Ussler and an anonymous reviewer for detailed and constructive reviews.

[26] The Editor thanks William Ussler and an anonymous reviewer for their assistance in evaluating this paper.

References

Bohannon, J. (2008), Weighing the climate risks of an untapped fossil fuel, *Science*, *319*(5871), 1753.

Bondarev, V., A. Dlugach, and S. Rokos (1999), Acoustic facies of post-cryogenic conditions at shallow areas of Pechora and Kara Seas, *Prospect and protection of mineral resources*, *7–8*, 10–14.

Bondarev, V., S. Rokos, D. Kostin, A. Dlugach, and N. Polyakova (2002), Underpermafrost accumulations of gas in the upper part of the sedimentary cover of the Pechora Sea, *Geol. Geophys.*, *43*(7), 587–598.

Brothers, L. L., P. E. Hart, and C. D. Ruppel (2012), Minimum distribution of subsea ice-bearing permafrost on the U.S. Beaufort Sea continental shelf, *Geophys. Res. Lett.*, *39*, L15501, doi:10.1029/2012GL052222.

Damm, E., U. Schauer, B. Rudels, and C. Haas (2007), Excess of bottom-released methane in an Arctic shelf sea polynya in winter, *Cont. Shelf Res.*, *27*(12), 1692–1701.

GEOS (1997), Batdaratskaya Bay enviromental conditions, in *The Basic Result of Studies for the Pipeline "Yamal-Center" Underwater Crossing Design*, GEOS, Moscow, pp. 432.

Greinert, J., D. F. McGinnis, L. Naudts, P. Linke, and M. De Batist (2010), Atmospheric methane flux from bubbling seeps: Spatially extrapolated quantification from a Black Sea shelf area, *J. Geophys. Res.*, *115*, C01002, doi:10.1029/2009JC005381.

Hovland, M., and A. G. Judd (1988), *Seabed Pockmarks and Seepages*, Graham & Trotman, London, pp. 180–182.

Hunter, J. A., K. G. Neave, H. A. MacAulay, and G. D. Hobson (1978), *Interpretation of sub-seabottom permafrost in the Beaufort Sea, paper presented at Third International Conference on Permafrost*, Natl. Res. Counc. of Can, Edmonton, Alberta, Canada.

Khimenkov, A., and A. Brushkov (2003), Oceanic Cryolithogenesis, 336 pp., Nauka, Moscow.

Kopf, A. J. (2002), Significance of mud volcanism, *Rev. Geophys.*, *40*(2), 1005, doi:10.1029/2000RG000093.

Melnikov, V., and V. Spesivtsev (1995), Engineering-Geological Conditions of Barents and Kara Sea Shelves.

Merewether, R., M. S. Olsson, and P. Lonsdale (1985), Acoustically detected hydrocarbon plumes rising from 2-km depths in Guaymas Basin, Gulf of California, *J. Geophys. Res.*, *90*(B4), 3075–3085.

Paull, C., W. Ussler, S. R. Dallimore, S. M. Blasco, T. D. Lorenson, H. Melling, B. E. Medioli, F. M. Nixon, and F. A. McLaughlin (2007), Origin of pingo-like features on the Beaufort Sea shelf and their possible relationship to decomposing methane gas hydrates, *Geophys. Res. Lett.*, *34*, L01603, doi:10.1029/2006GL027977.

Paull, C., et al. (2011), Tracking the decomposition of permafrost and gas hydrate under the shelf and slope of the Beaufort Sea, in *7th International Conference on Gas Hydrate*, edited, p. 12.

Polikarpov, G. G., V. N. Egorov, A. I. Nezhdanov, S. B. Gulin, Y. D. Kulev, and M. B. Gulin (1989), The phenomenon of active gas escapes from mounts on the slope of the western Black Sea, *Dokl. AN UkrSSR*, *12-B*, 13–16.

Polyak, L., F. Niessen, V. Gataullin, and V. Gainanov (2008), The eastern extent of the Barents–Kara ice sheet during the Last Glacial Maximum based on seismic-reflection data from the eastern Kara Sea, *Polar Research*; *27*(2) (*2008*): *Special issue*: *Arctic Palaeoclimate and its Extremes* (*APEX*).

Rekant, P., and A. Vasiliev (2011), Distribution of subsea permafrost at the Kara Sea shelf, *Cryosphere of the Earth*, *XV*(4), 69–72.

Robinson, C. J., and J. Goómez-Gutieérrez (1998), The red-crab bloom off the west coast of Baja California, México, *J. Plankton Res.*, *20*(10), 2009–2016.

Rokos, S., D. Kostin, and A. Dlugach (2001), Free gas and permafrost in the upper deposits of shallow areas at Pechora and Kara Sea shelf, *Sedimentation processes and marine ecosystem evolution in marine periglacial conditions*, 40–51.

Romanovskii, N. N., and H. W. Hubberten (2001), Results of permafrost modeling of the lowlands and shelf of the Laptev Sea region, Russia, *Permafrost. Periglac.*, *12*(3), 191–202.

Shakhova, N., I. Semiletov, A. Salyuk, V. Yusupov, D. Kosmach, and Ö. Gustafsson (2010a), Extensive methane venting to the atmosphere from sediments of the East Siberian Arctic Shelf, *Science*, *327*, 1246–1250.

Shakhova, N., I. Semiletov, I. Leifer, A. Salyuk, P. Rekant, and D. Kosmach (2010b), Geochemical and geophysical evidence of methane release over the East Siberian Arctic Shelf, *J. Geophys. Res.*, *115*, C08007, doi:10.1029/2009JC005602.

Shearer, J. M., R. F. Macnab, B. R. Pelletier, and T. B. Smith (1971), Submarine pingos in the Beaufort Sea, *Science*, *174*(4011), 816–818.

Sherbakov, V., V. Motichko, and V. Konstantinov (2010), Estimation of background geological conditions of nearshore area and coastal zone at South-West Kara Sea for monitoring of bowels, *Report Rep. 504.4*:*556351*(*268*.*52*), 270 pp, VNIIOkeangeologia, Saint-Petersburg, Russia.

Skorobogatov, V. A., V. S. Yakushev, and E. M. Chuvilin (1998), Sources of natural gas within permafrost North-West Siberia, paper presented at Permafrost. Seventh International Conference. Proceedings, Canada, Canada.

Sloan, E. D. (1998), *Clathrate Hydrates of Natural Gases*, Taylor & Francis, New York.

Stupakova, A. (2011), Structure and petroleum potential of the Barents-Kara Shelf and adjacent territories, *Oil and gas geology*, *6*(6), 99–115.

Taylor, A. E. (1991), Marine transgression, shoreline emergence: Evidence in seabed and terrestrial ground temperatures of changing relative sea levels, Arctic Canada, *J. Geophys. Res.*, *96*(B4), 6893–6909.

Tréhu, A. M., P. B. Flemings, N. L. Bangs, J. Chevallier, E. Gràcia, J. E. Johnson, C. S. Liu, X. Liu, M. Riedel, and M. E. Torres (2004), Feeding methane vents and gas hydrate deposits at south Hydrate Ridge, *Geophys. Res. Lett.*, *31*, L23310, doi:10.1029/2004GL021286.

Vadakkepuliyambatta, S., S. Bünz, J. Mienert, and S. Chand (2013), Distribution of subsurface fluid-flow systems in the SW Barents Sea, *Mar. Pet. Geol.*, *43*(0), 208–221.

Westbrook, G. K., et al. (2009), Escape of methane gas from the seabed along the West Spitsbergen continental margin, *Geophys. Res. Lett.*, *36*, L15608, doi:10.1029/2009GL039191.

Wood, W. T., J. F. Gettrust, N. R. Chapman, G. D. Spence, and R. D. Hyndman (2002), Decreased stability of methane hydrates in marine sediments owing to phase-boundary roughness, *Nature*, *420*(6916), 656–660.